beta-Ta and alpha-Cr thin films deposited by high power impulse magnetron sputtering and direct current magnetron sputtering in hydrogen containing plasmas

Hans Högberg, Lina Tengdelius, Mattias Samuelsson, Jens Jensen and Lars Hultman

Original Publication:

Hans Högberg, Lina Tengdelius, Mattias Samuelsson, Jens Jensen and Lars Hultman, beta-Ta and alpha-Cr thin films deposited by high power impulse magnetron sputtering and direct current magnetron sputtering in hydrogen containing plasmas, 2014, Physica. B, Condensed matter, (439), 3-8.
http://dx.doi.org/10.1016/j.physb.2013.11.038

β-Ta and α-Cr thin films deposited by high power impulse magnetron sputtering and direct current magnetron sputtering in hydrogen containing plasmas

Hans Högberg[a,*], Lina Tengdelius[a], Mattias Samuelsson[b], Jens Jensen[a], and Lars Hultman[a]

[a]Department of Physics, Chemistry, and Biology (IFM) Linköping University, SE-581 83 Linköping, Sweden.

[b]Impact Coatings AB, Westmansgatan 29, SE-582 16 Linköping, Sweden

[*]Corresponding author. Electronic mail: hans.hogberg@liu.se

Abstract

Thin films of β-Ta and α-Cr were deposited on Si(100) and 1000 Å SiO_2/ Si(100), by high power impulse magnetron sputtering (HiPIMS) and direct current magnetron sputtering (dcMS) in hydrogen-containing plasmas. The films were characterized by X-ray photoelectron spectroscopy (XPS), X-ray diffraction, scanning electron microscopy, elastic recoil detection analysis, and four-point probe measurements. The results showed that 001-oriented β-Ta films containing up to ~8 at% hydrogen were obtained with HiPIMS, albeit with no chemical shift evident in XPS. The 110 oriented α-Cr films display a hydrogen content less than the detection limit of 1 at%, but H_2 favors the growth of high-purity films for both metals. The β-Ta films deposited with dcMS are columnar, which seems independent of H_2 presence in the plasma, while the films grown by HIPIMS are more fine-grained. The latter type of microstructure was present for the α-Cr films and found to be independent on choice of technique or hydrogen in the plasma. The β-Ta films show a resistivity of ~140-180 μΩ cm, while α-Cr films exhibit values around 30 μΩ cm; the lowest values obtained for films deposited by HiPIMS and with hydrogen in the plasma for both metals.

Keywords: Hydrides, thin films, β-Ta, α-Cr, high power impulse magnetron sputtering, direct current magnetron sputtering

1. Introduction

The d-block elements Zr, Ta, and Cr have been reported to form hydrides as bulk materials, albeit at different temperatures and H_2 pressures. For instance, when the group 4 element Zr in powder form is treated in 1 atmosphere of H_2 at 550 ^{o}C during 2 days, the phase δ-ZrH_2 (fcc, CaF_2-type structure) is formed [1]. This hydride is stable to ~700-800 ^{o}C according to the phase diagram, but from literature data the transformation temperature is uncertain [2]. Moving to group 5 and the metal Ta, the hydride formation is more restricted to temperatures below or close to room temperature [2, 3] and with reported phases such as hexagonal β-Ta_2H [4] and orthorhombic $TaH_{0.93}$ [5]. The group 6 transition metal Cr is able to form hydrides with 1:1 Cr to H composition, but at a combination of high temperatures > 1000 ^{o}C and at extreme hydrogen pressure of 5.5 GPa [6]. At these conditions the metal forms two phases, one with hexagonal symmetry (hcp) and another with cubic symmetry (fcc) [6].

From the above reports, it is obvious that the transition metals Zr, Ta, and Cr interact differently with hydrogen. The trend for stability of the formed hydrides is decreasing when going from left to right in the periodic chart, which indicates a decreasing affinity to hydrogen in the order: Zr, Ta, and Cr. From this observation, we highlight the trend with an increasing electronegativity (χ) going from group 4 to group 6 with Zr, χ= 1.33, Ta, 1.5, and Cr, 1.66 according to the Pauling scale [7]. Given the more electronegative nature of H with 2.2 on the Pauling scale [7] the element will act as an electron acceptor to Zr, Ta, and Cr when forming a compound such as a hydride. Furthermore, the difference in electronegativity between the metal and hydrogen will determine the degree of electron transfer from the metal to hydrogen when forming a hydride, where a large difference is favorable for electron transfer. This

suggests that hydride formation should be easiest for Zr and less expected for Cr, which is in agreement with the reports above. However, the fact remains that hydrides of Ta and Cr have been synthesized. Thus, there may be alternative synthesis techniques and/or routes to grow these phases.

Thin film growth techniques such as high power impulse magnetron sputtering (HiPIMS) [8] and direct current magnetron sputtering (dcMS) are characterized by growth of materials far from thermal equilibrium. The energetic growth flux of ions in HiPIMS or neutrals in dcMS should therefore be favorable in the synthesis of Ta, Cr as well as other hydrides such as δ-ZrH_2 [1, 2] that are previously unstudied as thin film materials. A further advantage is the fact that films are built more or less atom-by-atom, which results in a material with well-defined properties. This is favorable to establish necessary synthesis-structure-property-relationships for these hydrides.

In this study, we investigate reactive sputtering of Cr and Ta films in hydrogen containing plasmas, using HiPIMS and dcMS and growth in an industrial scale deposition system. The deposition were performed without external heating to avoid decomposition of potential low-temperature stable phases, using short deposition time and high power density on the target to minimize the influence of the residual gas during growth. The deposited films were investigated with respect to their chemical bonding structure, composition, structural properties, microstructure, and electrical properties.

2. Material and methods

The thin film growth was carried out in a commercial industrial high vacuum (HV) coating system (CemeCon CC800/9®) at a fixed target to substrate distance of 7 cm and with no external substrate heating. Prior to deposition the chamber was evacuated to a base pressure below 2.3×10^{-4} Pa and to further lower the impact of the residual gas, sputtering of a titanium

target was performed immediately before growth onto a shutter that covered the magnetron, using an effect of 1500 W during 600 s and at a pressure of 0.42 Pa. The Cr films were sputtered from a chromium target with a purity of >99.9% on Si(100) substrates, two in each run, while the Ta films were deposited from a tantalum target (99.5% purity) onto Si(100) and 1000Å SiO_2/ Si(100) substrates. Growth by HiPIMS or dcMS were conducted at a substrate bias of - 80 V and with the Ar partial pressure set to 0.42 Pa for Ar/H_2 plasmas containing 0, 2.5, 5, 10, 15, and 20% H_2 as seen from the resulting total pressure at the beginning of the deposition cycle. As no pressure control was applied for H_2 during growth, the pressure increased during growth in particular for the HiPIMS processes performed with high hydrogen contents in the plasma. The power to the cathode, after ramping of the target effect behind a shutter, was set to 5000 W (11.36 W/cm^2) for dcMS and with a 3000 W (6.82 W/cm^2) average constant power during HiPIMS, using a pulse width of 150 μs and a pulse repetition frequency of 300 Hz. The deposition time for the Cr films was set to 60 s for the dcMS processes and 248 s for the HiPIMS processes, while the Ta films were grown for 138 s and 570 s, for the two techniques respectively. The deposition times were selected to deposit films with similar thicknesses, using both techniques.

The chemical bonding structure present in the films was investigated by X-ray photoelectron spectroscopy (XPS), using an AXIS Ultra^{DLD} instrument from Kratos Analytical and analysis with monochromatic Al Kα radiation. The binding energy (BE) scale was calibrated by setting the position of the Fermi edge of a sputter-cleaned Ag sample to 0.0 eV [9]. The samples were sputter-cleaned by 4 kV Ar^+ at an angle of 20^o for 60 s to remove adsorbed contaminants following exposure to the air. To evaluate the amount of hydrogen incorporated in the Cr and Ta films as well as the level of contaminants in the Cr films, selected samples were investigated by elastic recoil detection analysis (ERDA). For the Cr samples, time-of-flight energy (ToF-E) ERDA with 36 MeV $^{127}I^{8+}$ ions as projectiles was applied to obtain the

elemental depth profiles. The ion incident angle relative to the surface normal was 67.5° and the detector was positioned at a recoil angle of 45°. A detailed description of the experimental set-up has been given elsewhere [10, 11]. For the Ta samples, the hydrogen content was assessed by conventional ERDA using 3.0 MeV $^4He^+$ ions as the primary beam. An absorbing aluminium foil with a thickness of 10 μm was used in front of the energy detector to filter out He^+ ions forward scattered due to the heavier elements. The incident angle of primary ions was 70° to the sample surface normal and the recoil angle was 40°. A reference sample with known H content was used for calibration of the data in both types of ERDA measurements. The phase distributions of the films were characterized by X-ray diffraction (XRD) θ/2θ scans in a Philips powder diffractometer, using Cu Kα radiation at 40 kV and 40 mA. The film microstructures and thicknesses were investigated by cross-sectional scanning electron microscopy (SEM, LEO 1550 Gemini) operated at an acceleration voltage of 10 kV. All samples were cooled using liquid nitrogen prior to cleaving. The electrical resistivity values of the films were calculated from measured sheeth resistivity data determined from four point probe measurements Model 280C (Four dimensions) instrument and using the film thicknesses from SEM images.

3. Results and discussion

3.1 Chemical bonding structure and composition

The high-resolution XPS spectra in Fig. 1 are obtained from the Cr 2p and Ta 4f photoelectron regions: in Fig.1a from a Cr-H film deposited by HiPIMS with 20% H_2 in the plasma (solid line) and from Cr reference film grown by HiPIMS in pure Ar plasma (dashed line) and in Fig. 1b from of a Ta-H film deposited by HiPIMS with 20% H_2 in the plasma (solid line) and from Ta reference film grown by HiPIMS in pure Ar plasma (dashed line). As can be seen, no chemical shifts are evident in the spectra recorded from both metals. This is in

contrast to the chemical shift of 0.5 eV of the Zr $3d_{5/2}$ peak to higher BE found from analysis of synthesized δ-$ZrH_{1.9}$ compared to Zr powder [1]. This result suggests that both Ta and Cr interacts weakly with hydrogen, but does not rule out the possibility that hydrogen is present in the films as XPS is unable to qualitatively and quantitatively determine hydrogen. For such investigations, we applied ERDA and the measurements show that less than 1 at% hydrogen is present in Cr films as this amount is the detection limit for the technique. In contrast, ~8 at% of hydrogen was found in the Ta films deposited with HiPIMS and 20% H_2 in plasma, while only ~4 at% hydrogen was found in the corresponding dcMS film and with a background level of ~1 at% established from both Ta reference films. A possible explanation for this behavior is the longer deposition time applied during growth with HiPIMS, which is likely to favor diffusion of hydrogen into the film. The importance of hydrogen during growth is further supported from measurements of HiPIMS films deposited with 2.5 at% that show ~4 at% hydrogen, which is in agreement with expectations that the amount of hydrogen in the films scales with the H_2 content in the plasma. The fact that higher amounts of hydrogen were found in the Ta films compared to the Cr films provides further support that Ta exhibits a higher affinity to hydrogen given its lower electronegativity value. This suggests that Ta chemically interacts with H, but that the amount of hydrogen present in the structure is too low to yield a chemical shift in XPS and/or that the shift is very small as the chemical shift in bulk δ-$ZrH_{1.9}$ was only ~0.5 eV for the more electropositive metal Zr [1].

In addition, from the peak positions in Figure 1 it was possible to determine the chemical bonding in the investigated films. The measured positions with the Cr 2p peaks at Cr $2p_{3/2}$ = 574.5 eV and Cr $2p_{1/2}$ = 583.7 eV and with the Ta 4f peaks at Ta $4f_{7/2}$ = 21.9 eV and Ta $4f_{5/2}$ = 23.8 eV are all in excellent agreement with data established for metal-metal bonding in Cr and Ta [12]. In addition, the recorded high-resolution spectra from the elements C, and N exhibit no visible peaks or in the case for O peaks of very weak intensity after 60 s of sputter-

cleaning. This show that the bulk of the films is of high purity, which is further supported from the fact that lighter elements such as O is typically concentrated during sputter-cleaning with Ar^+. The growth of high-purity Ta and Cr films could be confirmed by ToF-E ERDA, where the measurements of the Cr films showed N content of 0.1 at% and with slightly higher O and C contents; typically < 0.2 at% for O and of 0.3-1at%, where the highest levels encountered in films deposited with dcMS and the lowest value found for our HiPIMS film growth with 20% H_2 in plasma. The latter observation is also supported from ToF-E ERDA measurements of Zr-H films showing a low O content of < 0.2 at% in the deposited films when H_2 is added to the plasma. This suggests that H_2 chemically interacts with species from the residual gas present on the film surface during growth and that hydrogen decreases the level of contaminants in the deposited films. Here we note that hydrogen is frequently applied in chemical vapor deposition processes to reduce halide-based precursors [13] and to chemically etch excess carbon [14] by forming volatile species with the contaminants, thus allowing them to be removed from the growing films in the form of gaseous molecules.

3.2 Structural properties

The XRD patterns in Fig. 2 are recorded from Ta films deposited by HiPIMS on Si(100) substrates, with a reference film displayed in the lower diffractogram and with films grown with 10% and 20% H_2 in the plasma shown in the middle and upper diffractogram, respectively. As can be seen, all films exhibit peaks at the diffraction angles $2\theta \approx 17^o$, 34^o, 52^o, and 120^o, where the peak at 34^o shows the highest intensity excluding the substrate 400 peak at 69^o. These peaks originate from β-Ta, which is a metastable phase of tetragonal crystal symmetry that is frequently found for Ta films grown by HiPIMS [15] and dcMS [16]. The peaks from low to high 2θ angles can be assigned to the 001, 002, 003, and 006 planes of β-Ta, where the expected 004 peak at 71^o is probably overlapping with the Si 400 peak and the 005 peak that should be visible at 93^o is reported to be of low intensity and therefore absent

[16]. In addition, there is a peak of low intensity located at 38^{o} that is best visible for the Ta reference film. The peak is the 110 peak from the stable bcc phase of the metal, α-Ta. Growth of this phase is typically favored at elevated temperatures and/or on special substrates [16, 17], which is probably the main reasons why α-Ta films are not obtained in this study.

The fact that only peaks of the 00ℓ type are found in the diffractogram indicates that the films are either epitaxial or textured; the misfit to the Si(100) substrate is - 2.2% for 001 plane of β-Ta. However, we suggest that our films are 001 textured as films deposited on 1000Å SiO_2/Si(100) substrates display 00ℓ peaks with comparable intensities to those recorded for films grown on Si(100). Furthermore, a closer inspection of the 002 peak showed a shift to lower diffraction angles when hydrogen is added to the plasma, see inset in Fig. 2. The shift was also present for films deposited on 1000Å SiO_2/Si(100) substrates. This observation suggests a larger spacing between the planes, which is most likely an effect of compressive stresses in the films given the intense ion bombardment characteristics for the HiPIMS technique [8]. We also note the difference in hydrogen content between the films with the ~1 at.%, i.e. background concentration, measured for the reference film and the 8 at.% found in the film deposited with 20% H_2 in the plasma.

Furthermore, analysis of films deposited by dcMS on Si(100) and 1000Å SiO_2/ Si(100) substrates showed that 001 oriented β-Ta films could also be grown by this technique, see Fig. 3 for films deposited on Si(100) and with a Ta reference film as the lower pattern and a film grown with 20% H_2 in the plasma as the upper pattern. As can been seen the 004 peak is now resolved from the Si 400 peak. The sharper peaks of lower full-width at half maximum and the change in peak positions for the β-Ta 00ℓ peaks to higher diffraction angles indicate a lower level of stress in the films deposited by dcMS compared to those grown by HiPIMS, but again noting the difference in hydrogen content in films grown by the two techniques. In

addition, the fact that the 001 and 003 peaks are present in our diffraction patterns provides support to the conclusion made in [16], showing the space group of β-Ta to be P-42_1m rather than the previously suggested $P4_2$/mnm [18].

Finally, diffraction analysis of the deposited Cr films showed that 110 oriented films of the stable bcc phase α-Cr was obtained and with no difference in growth behavior encountered for films grown with or without H_2 in the plasma or with HiPIMS or dcMS. Such texture is to be expected in sputtering of bcc metals such as Cr, see e.g. [19] and the growth condition is favored in dcMS by low substrate temperatures and at low substrate bias voltages [20] such as the conditions applied in our study.

3.3. Microstructure

The SEM cross-section images in Fig. 4 were obtained from β-Ta films deposited with HiPIMS for (a) a reference film and (b) a film grown with 20% H_2 in the plasma, and with dcMS for (c) a reference film and (d) a film that was processed with 20% H_2 in the plasma. From the images, a columnar growth is evident for the films deposited by dcMS whereas those grown with HIPIMS display a more fined grained microstructure, albeit with a tendency to broken columns. This growth behavior for the HiPIMS films is probably the reason for the peak broadening encountered in the diffractograms recorded compared to those seen for films deposited by dcMS as peak broadening in XRD is typically associated with a smaller grain size, see Figs. 2 and 3. The fine-grained microstructure is supported from several reports on thin film growth of metal films by HiPIMS, revealing a fine grained or even glass-like microstructure for films grown by the technique for e.g. deposition of Ta in [21] and growth of Ti in [22]. Furthermore, from the images it is not possible to discern any pronounced difference in microstructure between the films grown with 20% H_2 in the plasma and their corresponding reference film. This is an indication that hydrogen has little or no impact on the

microstructural evolution of β-Ta films grown either by HiPIMS or dcMS, which finds support from the low amounts of the element that is incorporated into the films and in particular for films deposited by dcMS. In addition, the film thicknesses can be estimated from the images, to be in the range ~590-630 nm, independently of the amount of hydrogen in the plasma for the films grown with HiPIMS, whereas the dcMS films were slightly thicker with values in the range ~640-690 nm and following the same behavior as the HiPIMS films with respect to dependence on H_2 in the plasma. The corresponding growth rates could be determined to 1.1 nm/s for the films grown by HiPIMS and more than four times higher for the films deposited by dcMS seen from a growth rate of 4.8 nm/s.

The SEM investigation showed that the α-Cr films were considerably thinner than the β-Ta films with thicknesses in the range of ~370-410 nm for HiPIMS films and similar values were found for the dcMS films with thicknesses in the range of ~350-420 nm, see Fig. 5. For the films deposited with dcMS there was a trend with a decreasing film thicknesses at increasing H_2 content in the plasma, while no such trend was found for the films grown by HiPIMS. In spite of lower thickness values the corresponding growth rates were higher compared to Ta for both the HiPIMS films with 1.6 nm/s and the dcMS films with 6.3 nm/s. The explanation is the higher sputter yield for Cr compared to Ta, with 1.1 atom/ Ar ion for Cr and 0.4 atom/ Ar ion for Ta at an ion energy of 400 V [23], albeit using shorter deposition time with 248 s for HiPIMS and 60 s for dcMS The images show no pronounced difference in microstructure between the films deposited by HiPIMS and dcMS or with or without H_2 in the plasma as all investigated films show similar fine grained microstructure with tendency to form columns. The reason for this behavior could be the higher sputter yield of Cr compared to Ta, which leads to fast nucleation at the applied growth conditions that are characterized by low surface mobility as no external heating was applied.

3.4 Resistivity

Four-point probe measurements showed that the deposited α-Cr and β-Ta films were metallic conductors. All α-Cr films display resistivity values ~30 μΩ cm irrespective of deposition technique and if hydrogen has been added to the plasma or not, but with the lowest values determined for films deposited by HiPIMS and with hydrogen in the plasma. Here, we note that these films exhibited a low level of contaminants according to the ToF-E ERDA measurements, supporting properties of hydrogen in decreasing the incorporation of contaminants during film growth. The resistivity values obtained are about double that of bulk α-Cr with a resistivity of 12.9 μΩ cm [24]. This can be expected as thin films generally display a higher resistivity values due to a more pronounced surface scattering.

The β-Ta films showed resistivity values in the range of ~140-180 μΩ cm, which is in agreement with previous studies reporting values of 180- 220 μΩ cm, see review in [17]. These values are about ten times higher than for of bulk α-Ta with a resistivity of 13.1 μΩ cm [24] and reflect the electrical properties of β-Ta films. Consequently, the high resistivity value of β-Ta films constitutes a limitation in applications envisioned for Ta films as, for instance, high temperature stable conductive films. As for the metal Cr, the lowest values were measured for films deposited by HiPIMS and using hydrogen in the plasma. In contrast, the films grown by dcMS showed slightly higher resistivity values when hydrogen was added to the plasma. This suggests that the shorter deposition time of 138 s applied for growth by dcMS compared to 570 s applied in HiPIMS provides hydrogen with shorter time to chemically remove contaminants from the growing film.

4. Conclusions

Our study shows that sputtering of Ta and Cr in a H_2-containing plasma by the HiPIMS and dcMS techniques results in the growth of 001 oriented β-Ta films on bare and SiO_2-covered Si(100) wafer substrates, and 110-oriented α-Cr films deposited on Si(100). The β-Ta films contain up to 8 at% of hydrogen when grown with HiPIMS using 20% H_2 in the plasma. While the amount of hydrogen in the as-deposited Cr films is below the detection limit, the hydrogen in the discharge favors growth of films with a very low level C, N, and O with less than 0.2 at% of oxygen determined for the Cr films. The β-Ta films deposited by dcMS exhibit a columnar microstructure independent of H_2 in the plasma, while the films grown with HiPIMS display a more fine-grained microstructure characteristic to this technique. The resistivity of the β-Ta films is in the range of ~140-180 μΩ cm and agrees with previously reported values, while the Cr films exhibit a lower resistivity of ~30 μΩ cm, i.e. twice that of the bulk metal.

Acknowledgments

Dr. Lars-Åke Näslund is gratefully acknowledged for assistance with the XPS measurements. HH acknowledges financial support from the Swedish Research Council (VR) through the Contract 622-2008-1247 and the Swedish Government Strategic Research Area in Materials Science on Functional Materials at Linköping University (Faculty Grant SFO-Mat-LiU # 2009-00971). LH and JJ acknowledge the Linköping Linnaeus Initiative LiLi-NFM, supported by the VR Grant 2008-6572. The authors are grateful for access to the Tandem Laboratory at Uppsala University.

References

[1] J.D. Corbett, H.S. Marek, Inorg. Chem. 22 (1983) 3194.

[2] T.B. Massalski, J.L. Murray, L.H. Bennett, H. Baker, Binary Alloy Phase Diagrams, American Society for Metals, Metals Park, Ohio, USA (1986).

[3] J. Köbler, J.-M. Welter, J. Less-Common Met. 84 (1982) 225.

[4] International Centre for Diffraction Data, Tantalum Hydride (β-TaH_2), PDF no: 03-0923.

[5] International Centre for Diffraction Data, Tantalum Hydride ($TaH_{0.93}$), PDF no: 39-1329.

[6] Y. Fukai, M. Mizutani, Mater. Trans. (Jap), 43 (2002) 1079.

[7] A.L. Allred, J. Inorg. Nucl. Mater., 17 (1961) 215.

[8] K. Sarakinos, J. Alami, S. Konstantinidis, Surf. Coat. Technol. 204 (2010) 1661.

[9] S. Hüfner, Photoelectron Spectroscopy: Principles and Applications, third ed. Springer-Verlag: Berlin, Germany, 2010.

[10] H.J. Whitlow, G. Possnert, C.S. Petersson, Nucl. Instrum. Methods Phys. Res. Sect. B: Beam Interact. Mater. At. 27 (1987) 448.

[11] J. Jensen, D. Martin, A. Surpi, T. Kubart, Nucl. Instrum. Methods Phys. Res. Sect. B: Beam Interact. Mater. At. 268 (2010) 1893.

[12] J.F. Moulder, W.F. Stickle, P.E. Sobol, K.D. Bomben, in: J. Chastain (Ed.), Handbook of X-ray Photoelectron Spectroscopy, Perkin-Elmer Corporation, Physical Electronics Division, Eden Prairie, MN, USA, 1992.

[13] W. Kern, V.S. Ban, in: J.L. Vossen, W. Kern (Eds.), Thin Film Processes, Academic Press, Inc, New York, NY, USA, 1978, pp. 257-331.

[14] P.E. Pehrsson, F.G. Celii, J.E. Butler, in: R.F. Davis (Ed.), Diamond Film and Coatings, Noyes Publications, Park Ridge, NJ, USA, 1993, pp. 68-146.

[15] J. Alami, P. Eklund, J.M. Andersson, M. Lattemann, E. Wallin, J. Bohlmark, P. Persson, U. Helmersson, Thin Solid Films 515 (2007) 3434.

[16] A. Jiang, T.A. Tyson, L. Axe, L. Gladczuk, M. Sosnowski, P. Cote, Thin Solid Films 479 (2005) 166.

[17] P.N. Baker, Thin Solid Films, 14 (1972) 3.

[18] P.T. Moseley, C.J. Seabook, Acta Crystallogr. B 29 206 (1973) 1170.

[19] H.J. Lee, J. Appl. Phys., 57 (1985) 4037.

[20] C. Paturaud, G. Farges, M.C. Sainte Catherine, J. Machet, Thin Solid Films, 347 (1999) 46.

[21] J. Alami, P.O.Å. Persson, D. Music, J.T. Gudmundsson, J. Bohlmark U. Helmersson, J. Vac. Sci. Technol. A 23 (2005) 278.

[22] M. Samuelsson, D. Lundin, J. Jensen, M.A. Raadu, J.T. Gudmundsson, U. Helmersson, Surf. Coat. Technol. 205 (2010) 591.

[23] N. Matsunami, Y. Yamamura, Y. Itikawa, N. Itoh, Y. Kazumata, S. Miyagawa, K. Morita, R. Shimizu, H. Tawara, At. Data Nucl. Data Tables, 31 (1984) 1.

[24] C. Kittel, Introduction to Solid State Physics, seventh ed., John Wiley & Sons Inc., New York, NY, USA (1996)

Figure captions

Figure 1. High-resolution XPS spectra of (a) Cr 2p from a Cr-H film deposited by HiPIMS with 20% H_2 in the plasma (solid line) and a Cr reference film grown by HiPIMS (dashed line), and (b) Ta 4f from of a Ta-H film deposited by HiPIMS with 20% H_2 in the plasma (solid line) and Ta reference film grown by HiPIMS (dashed line).

Figure 2. X-ray θ/2θ scans of: a Ta reference film grown by HiPIMS (lower pattern), a Ta film deposited by HiPIMS and with 10% H_2 in the plasma (middle pattern), and a Ta film deposited by HiPIMS and with 20% H_2 in the plasma (upper pattern). The inset shows the 2θ region around the 002 peak for the deposited films.

Figure 3. X-ray θ/2θ scans of: a Ta reference film grown by dcMS (lower pattern) and a Ta films deposited by HiPIMS and with 20% H_2 in the plasma (upper pattern).

Figure 4. SEM images obtained from β-Ta films, (a) 600 nm thick reference film deposited by HiPIMS, (b) 620 nm thick film deposited by HiPIMS and with 20% H_2 in the plasma, (c) 660 nm thick reference film deposited by dcMS, and (d) 650 nm thick film deposited by dcMS and with 20% H_2 in the plasma.

Figure 5. SEM images obtained from α-Cr films, (a) 410 nm thick reference film deposited by HiPIMS, (b) 400 nm thick film deposited by HiPIMS and with 20% H_2 in the plasma, (c) 420 nm thick reference film deposited by dcMS, and (d) 360 nm thick film deposited by dcMS and with 20% H_2 in the plasma.

Fig. 1

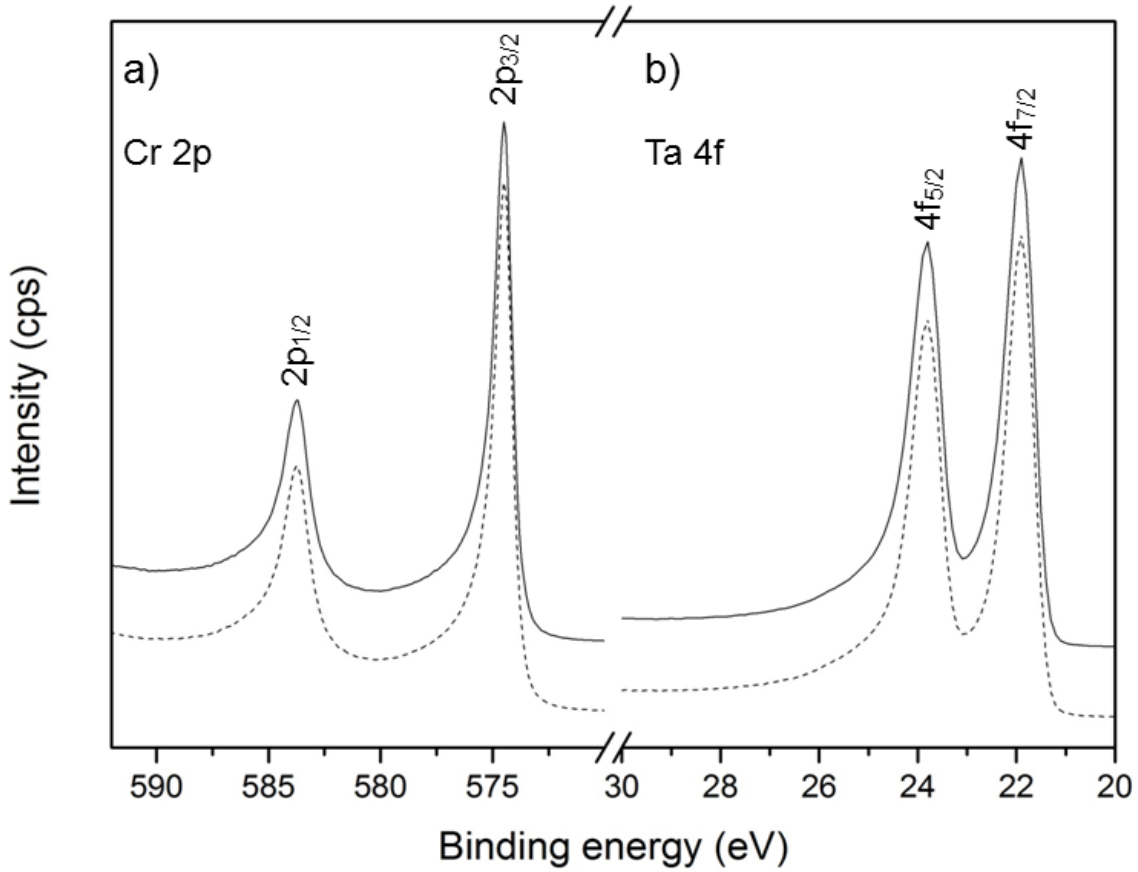
a)
Cr 2p
2p3/2
2p1/2
b)
Ta 4f
4f5/2
4f7/2
Intensity (cps)
590
585
580
575
30
28
26
24
22
20
Binding energy (eV)

Fig. 2

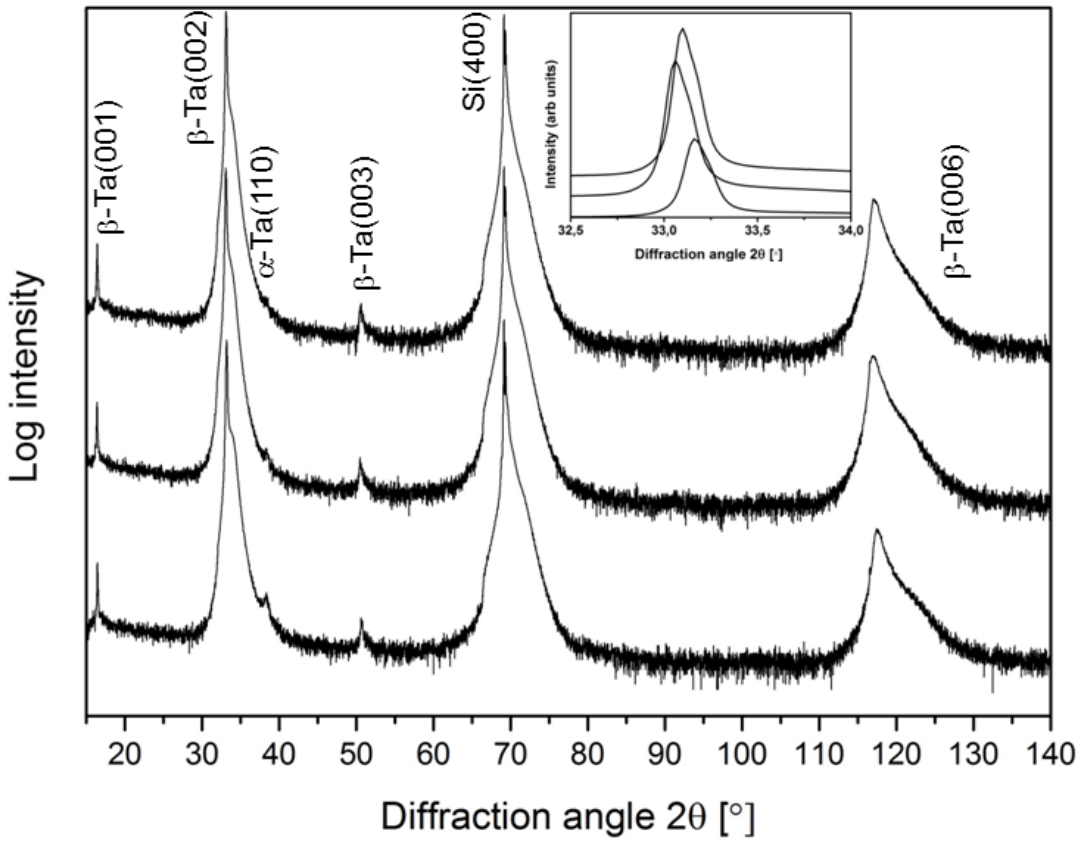
β-Ta(001)
β-Ta(002)
α-Ta(110)
β-Ta(003)
Si(400)
β-Ta(006)
Log intensity
20
30
40
50
60
70
80
90
100
110
120
130
140
Diffraction angle 2θ [°]
Intensity (arb units)
32,5
33,0
33,5
34,0
Diffraction angle 2θ [°]

Fig. 3

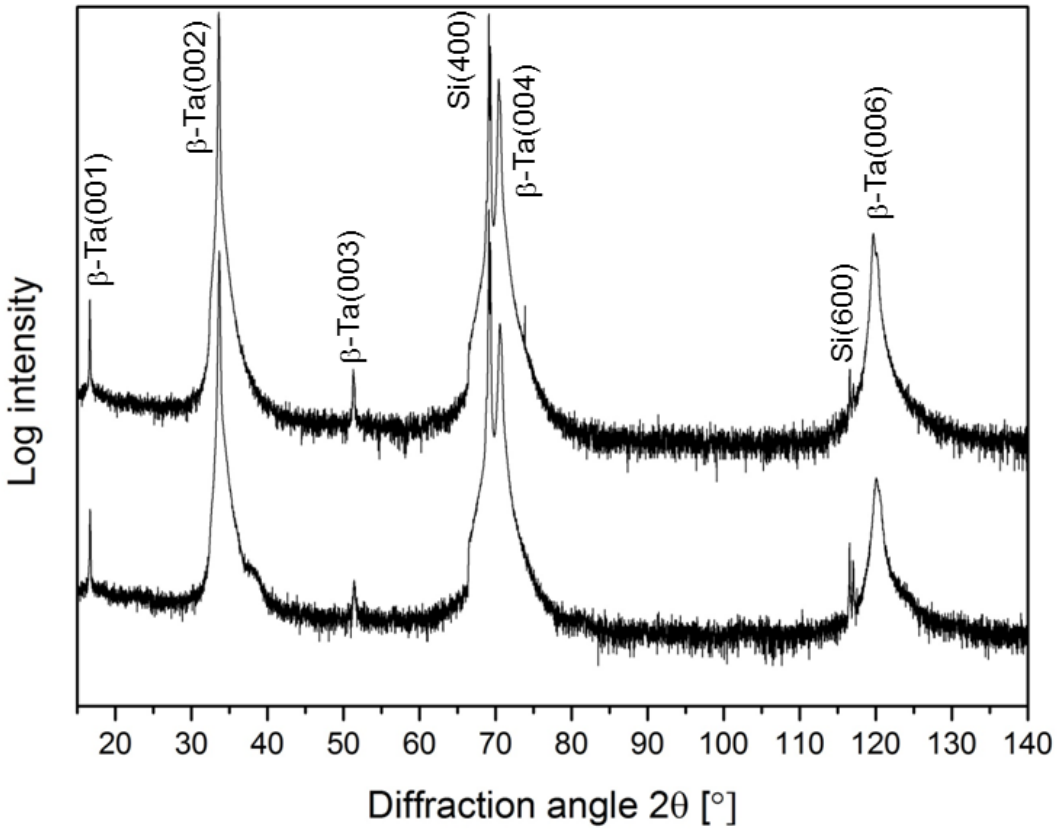
β-Ta(001)
β-Ta(002)
β-Ta(003)
Si(400)
β-Ta(004)
Si(600)
β-Ta(006)
Log intensity
20
30
40
50
60
70
80
90
100
110
120
130
140
Diffraction angle 2θ [°]

Fig. 4

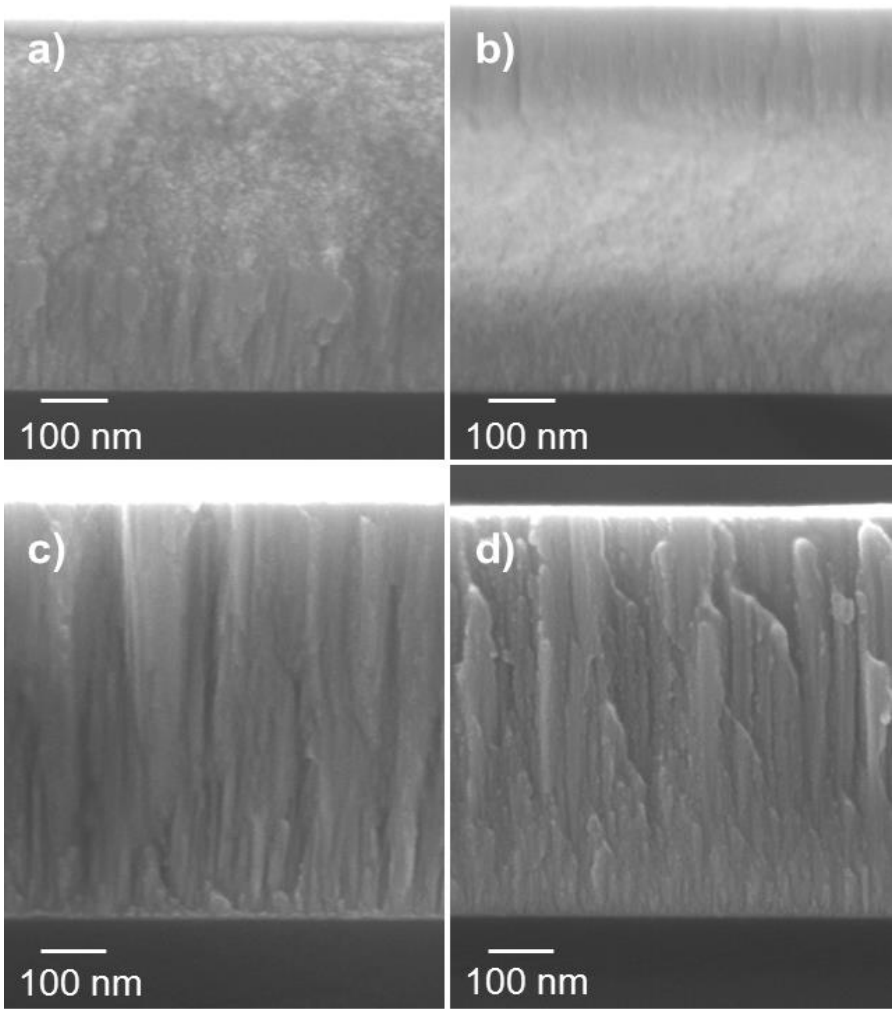

Fig. 5